ELSEVIER

Meat Science 57 (2001) 299–310

MEAT SCIENCE

www.elsevier.com/locate/meatsci

Two-dimensional visible/near-infrared correlation spectroscopy study of thawing behavior of frozen chicken meats without exposure to air☆

Yongliang Liu, Yud-Ren Chen *

Beltsville Agricultural Research Center, ARS, USDA, Beltsville, MD 20705-2350, USA

Received 19 May 2000; received in revised form 3 August 2000; accepted 3 August 2000

Abstract

The thawing behavior of frozen chicken meats without exposure to air was investigated by generalized 2D Vis/NIR correlation spectroscopy. The synchronous 2D visible correlation analysis revealed that intensities of the 435 and 555 nm bands increase, because of the relaxation of DeoxyMb and OxyMb components, whereas those of the 475 and 620 nm bands decrease as MetMb and SulfMb decompose into small molecules due to specific enzymes. The corresponding asynchronous spectra indicated that the decomposition of MetMb and SulfMb species precedes the recovery of DeoxyMb and OxyMb, and that the DeoxyMb species recovers faster than the OxyMb. Further, the asynchronous 2D NIR spectra suggested that the melting of ice crystals and the relaxation and proteolysis of proteins occurs earlier, indicating a coordination process for hydrophilic O–H and N–H groups. Moreover, strong correlation peaks correlating the bands in the visible and NIR spectral regions were observed and discussed. Published by Elsevier Science Ltd.

Keywords: Two-dimensional correlation analysis; Vis/NIR spectroscopy; Frozen meat; Chicken meat; Thawing

1. Introduction

Both the importance of freezing of meats and the proper procedures for freezing have been considered widely (Kinsman, Kotula & Breidemstein, 1994; Lawrie, 1985; Price & Schweigert, 1987). However, the subject of thawing, the opposite process to freezing, has been largely ignored. Generally, thawing increases molecular mobility, resulting in the relaxation of meat components frozen in a rigid state. Such relaxation may sometimes allow the reabsorption of the fluids (soluble proteins, vitamins, and salts) by the meat, but with a risk of meat discoloration and lipid oxidation if the thawing time is too long (Kinsman et al., 1994).

Visible/near-infrared (Vis/NIR) spectroscopy has found considerable application in safety and quality control issues of chicken meat products (Chen, Huffman, Park & Nguyen, 1996; Chen & Marks, 1997, 1998; Chen, Park, Huffman & Nguyen, 1998; McElhinney, Downey & Fearn, 1999; Rannou & Downey, 1997). Applications include the quantitative prediction of the physical characteristics of heat-treated chicken patties (Chen & Marks, 1997, 1998), the identification of the chicken species from other meats (McElhinney et al., 1999; Rannou & Downey, 1997), and the classification of chicken carcasses into wholesome and unwholesome classes at the slaughter plant (Chen et al., 1996, 1998). Moreover, generalized two-dimensional (2D) correlation analysis was recently applied to the Vis/NIR spectral region for the characterization of chicken meats with various treatments and conditions (Liu & Chen, 2000; Liu, Chen & Ozaki, 2000a,b). It has turned out that the 2D Vis/NIR approach can not only establish the spectral band assignments but also monitor the complex sequence of events arising from the changes in

☆ Mention of a product or specific equipment does not constitute a guarantee or warranty by the US Department of Agriculture and does not imply its approval to the exclusion of other products that may also be suitable.

* Corresponding author. Tel.: +1-301-504-8450; fax: +1-301-504-9466.

E-mail address: cheny@ba.ars.usda.gov (Y.-R. Chen).

0309-1740/00/$ - see front matter Published by Elsevier Science Ltd.
PII: S0309-1740(00)00106-6

meats during such processes as discoloration and tenderization.

In recent publications (Liu & Chen, 2000; Liu et al., 2000a), 2D Vis/NIR spectroscopic study was focused on both the cooking time- and the storage time-induced physical and chemical changes of chicken meats, in which the intervention of air was apparent. In the visible region, the significant spectral intensity reductions of the 445 and 560 nm bands revealed that both absorbances could be related to the discoloration of meats. Hence, the 445 and 560 nm bands have been assigned to deoxymyoglobin (DeoxyMb) and oxymyoglobin (OxyMb) components, which respectively are purplish and bright red in appearance (Kinsman et al., 1994; Lawrie, 1985; Price & Schweigert, 1987). The results also suggested that DeoxyMb and OxyMb degrade into metmyoglobin (MetMb), sulfmyoglobin (SulfMb), and small molecules through oxidation and reduction reactions. In addition, they showed that DeoxyMb, MetMb, and OxyMb components exist in all wholesome and unwholesome meats, with a clear indication that wholesome meats have more variation in OxyMb and DeoxyMb and less variation in MetMb than do diseased meats (Liu et al., 2000b).

The analysis of spectral intensity variations of the C–H and O–H/N–H vibration modes in the NIR region provided a very interesting point. It was observed that the intensity change of the C-H fractions occurs before those of the O–H/N–H groups for the chicken meats during cooking, but occurs after those of the O–H/N–H groups for the cold stored meats conditions (Liu & Chen, 2000; Liu et al., 2000a). Obviously, the reverse sequence of the C–H groups varying before/after the O–H/N–H groups suggested different mechanisms of chemical and biochemical reactions in the chicken meats corresponding to the external treatments. Possibly, the cooking of meats leads to the oxidization of lipids first, whereas the meats in cold storage first undergo denaturation and proteolysis of the proteins.

Our previous reports also indicated that intensity reduction of the visible bands due to DeoxyMb and OxyMb occurs before those of the NIR bands ascribed to the C–H and O–H/N–H vibrational modes, suggesting the possibility that the discoloration of meats precedes the other developments, such as tenderization (Liu & Chen, 2000; Liu et al., 2000a).

In the present study, the same strategy was applied to unravel the thawing behavior of frozen chicken meats without exposure to air, complementary to the previous investigation (Liu & Chen, 2000; Liu et al., 2000a). Vis/NIR spectra were measured over a time span of 0–180 min after the beginning of thawing, during which physical, chemical, and biochemical reactions could be induced by the melting of ice crystals and the increased mobility of meat components.

2. Materials and methods

2.1. Meat samples

Five wholesome fresh chicken carcasses were selected by a Food Safety and Inspection Service (FSIS) veterinarian from the processing line at a poultry slaughter plant located on the Eastern Shore of Maryland (Cordova, MD, USA). The carcasses, selected in the morning, were packaged into polyethylene bags which were then placed in a plastic cooler filled with ice, and transported to USDA's Instrumentation and Sensing Laboratory in Beltsville, MD. In the afternoon, five fresh breast meats (1 cm thick and 3.8 cm diameter) were cut from each of five chicken carcass, sized to fit into the spectrophotometer's quartz-windowed cylindrical cup. Then five cups with sliced meats inside were sealed in a polyethylene bag and stored in a freezer for 2–7 days until Vis/NIR measurements were taken.

2.2. Spectroscopic measurement and 2D correlation analysis

All the Vis/NIR reflectance spectra were recorded on a scanning monochromator NIRSystems 6500 spectrophotometer (NIRSystems, Silver Spring, MD, USA) equipped with a rotating sample cup. Each spectrum was collected over the 400–2500 nm wavelength range at 2 nm intervals, with 16 scans. The spectra of individual frozen meat samples were measured successively by a time increment of either 10 min (in the first 60 min) or 15 min after the beginning of thawing at room temperature, eventually producing 15 spectra over a time span of 180 min. Because the meat was covered by the quartz-window tightly, the thawing occurred without exposure to air.

Five spectra, collected for five frozen meats with the same thawing time, were averaged using Grams/32 software (Galactic Industrious Corp., Salem, NH, USA). Then the 15 averaged spectra, representing the thawing behavior of frozen meats, were loaded into the PLSPlus/IQ package in Grams/32 to perform principal component analysis (PCA). The PC scores–scores plot suggested two clusters of spectra: one consisted of seven spectra measured in the 0 to 60 min range and the other of eight spectra in the 75–180 min range. This small time range was taken to accentuate the thawing-time induced change of the Vis/NIR spectra.

The subsequent 2D correlation spectra of meats were derived from these two sets of Vis/NIR spectra by using the generalized 2D correlation analysis (Liu & Chen, 2000; Liu et al., 2000a,b; Noda, 1993). The principle for analyzing the positive/negative cross-peaks in synchronous and asynchronous spectra has been described by Noda. In a synchronous spectrum, positive peaks (shown in solid lines) indicate that intensity changes

observed at two spectral coordinates are in the same direction, while negative peaks (shown in dashed lines) mean that intensity changes are in opposite directions. Asynchronous peaks are used for evaluating the sequence of spectral intensity changes. A positive cross-peak indicates that the spectral intensity change observed at λ_1 occurs earlier than that at λ_2, and a negative peak indicates the opposite.

3. Results and discussion

3.1. Visible and NIR spectra of chicken meats

Fig. 1A and B, respectively, show the representative reflectance spectra in the spectral regions of visible 410–700 nm and NIR 1100–1850 nm of frozen chicken meats, recorded approximately at (a) 10, (b) 20, (c) 50, and (d) 105 min after the beginning of thawing. In this study, the carcasses were well-bled and thus myoglobin is the primary heme pigment in the meats (Fennema, 1996; Francis & Clydesdale, 1975; Liu et al., 2000b). Two broad visible bands centered at 430 and 555 nm are associated with various forms of myoglobin (Kinsman et al., 1994; Lawrie, 1985; Liu & Chen, 2000; Liu et al., 2000a,b; Price & Schweigert, 1987). In NIR region, bands between 1100 and 1300 nm are from the second overtones of the C–H stretching modes, and their first overtones appear in the 1600–1850 nm region (Liu & Chen, 2000; Liu et al., 2000a; Osborne, Fearn & Hindle, 1993; Williams & Norris, 1990). Features in the 1300–1400 nm region are ascribed to combination bands of the C–H vibrations. Broad bands in the 1400–1600 nm region are due to the first overtones of the O–H/N–H stretching modes of self-associated and water-bonded O–H/N–H groups in meat components. The thawing related time-dependent spectral intensity variation suggests both possible physical, chemical, and biochemical process and high scattering from crystal interfaces.

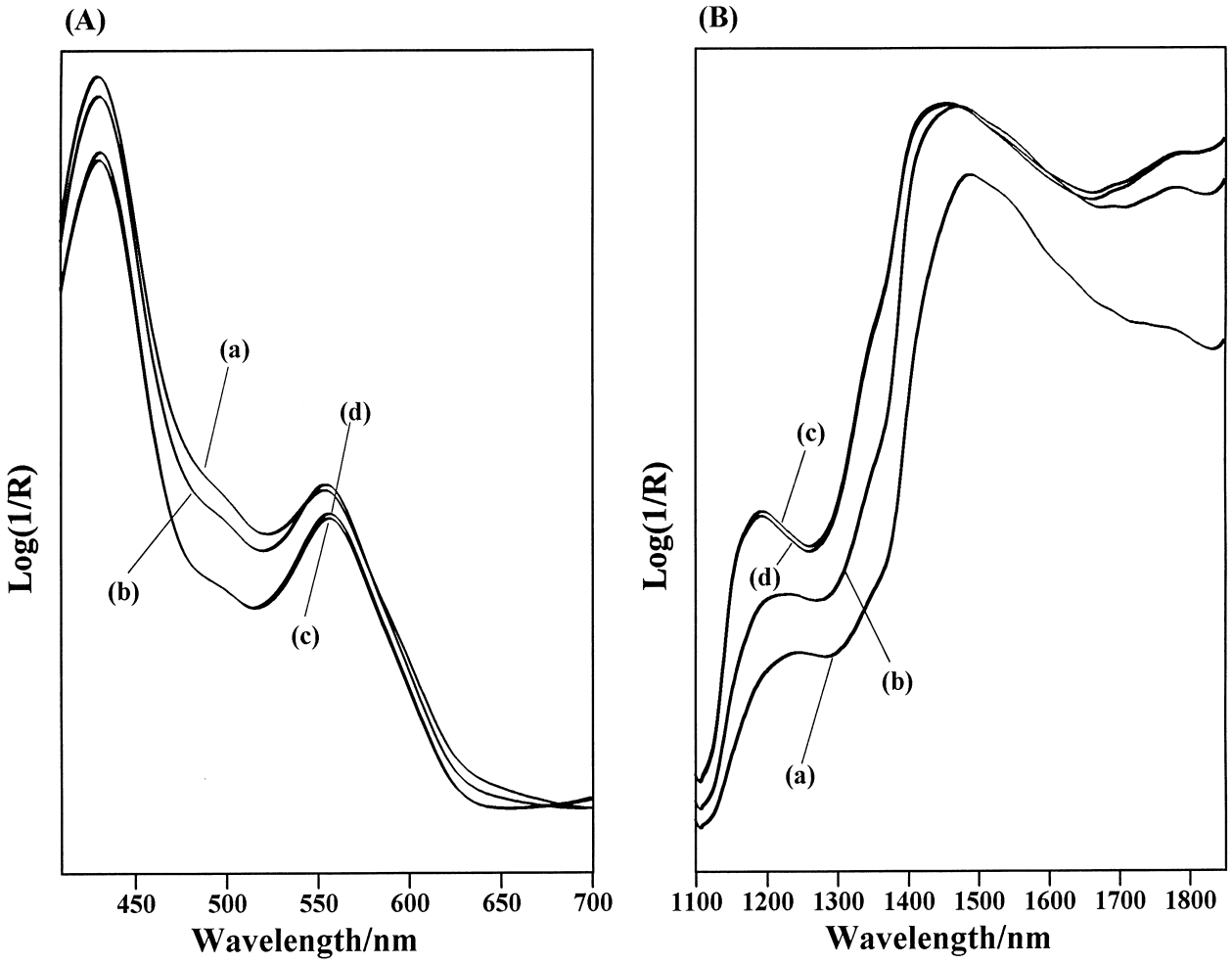

Fig. 1. Representative reflectance spectra in (A) 410–700 nm visible region and (B) 1100–1850 nm NIR region of frozen chicken meats recorded at (a) 10, (b) 20, (c) 50, and (d) 105 min after the beginning of thawing measurement.

3.2. 2D Correlation spectra in the visible region

Fig. 2a and b show, respectively, the synchronous and asynchronous 2D visible correlation spectra of frozen chicken meats measured from 0 to 60 min after the beginning of the thawing. One strong autopeak is observed at 475 nm in the synchronous spectrum (Fig. 2a), and it is clearly coupled with the 620 nm band. The presence of distinct positive cross-peaks (620 vs 475 nm) suggests that the spectral intensity change of the 475 band is in the same direction as that of the 620 nm band. The 475 and 620 nm bands can be assigned to the MetMb and SulfMb species, respectively, although they are approximately 10 to 15 nm lower than those reported in previous studies (Liu & Chen, 2000; Liu et al., 2000a,b). Notably, SulfMb is a comprehensive complex of Sulf-OxyMb, Sulf-DeoxyMb, and/or Sulf-MetMb. It will become clear in Fig. 6a that both bands reduce their intensities simultaneously. Hence, the reduction of MetMb and SulfMb species seems to result from the breakdown of both MetMb and SulfMb into small molecules (Liu & Chen, 2000; Voet & Voet, 1995). It is probably due to specific enzymes which are released from the frozen meats and activated during thawing.

In addition to the major autopeak, there is one minor autopeak appearing at 435 nm. It is due to the absorption of the DeoxyMb component (Liu & Chen, 2000; Liu et al., 2000a,b). Its appearance arises from the relaxation of the frozen heme pigment portion during the thawing process.

For the same time domain, the asynchronous spectrum shown in Fig. 2b reveals that either the 435 or 555 nm band is asynchronously correlated with two or three of the bands at 425, 475, and 620 nm. Notably neither autopeak nor cross-peak is observed near 555 nm in Fig. 2a, probably due to its minimal spectral intensity variation. The signs of asynchronous cross-peaks suggest that the intensity variation of the bands at 425, 475, and 620 nm occurs before that of the 555 nm band, and that the intensity variation of the 475 and 620 nm bands precedes that of the 435 nm band. The 555 nm absorbance has been ascribed to the OxyMb component (Liu & Chen, 2000; Liu et al., 2000a,b), while the 425 nm band to the Soret band for MetMb (Swatland, 1989). Consequently, Fig. 2b implies that the reduction of both MetMb and SulfMb species happens earlier than the relaxation of DeoxyMb and OxyMb components, suggesting that MetMb and SulfMb species decompose/degrade easily during the initial thawing.

Fig. 3a and b present, respectively, the synchronous and asynchronous 2D visible correlation spectra of frozen meats representing the thawing process from 75 to 180 min. The synchronous spectrum in Fig. 3a differs from the map in Fig. 2a covering the initial thawing period. It shows two major autopeaks at 435 and 555 nm, and several cross-peaks coordinated at 435 nm. The apparent appearance of the autopeaks at 435 and 555 nm probably reflects the continuous relaxation of DeoxyMb and OxyMb species in meats. Hence, proper thawing procedure might benefit the recovery of meat color, because the freezing preservation causes an undesirable color change (Kinsman et al., 1994).

The asynchronous spectrum in Fig. 3b reveals a complex feature, echoing the conclusion that each of DeoxyMb, OxyMb, and MetMb absorbs at several wavelengths due to the contribution of different chemical and physical environment to the heme portions (Liu & Chen, 2000). The positive asynchronous cross-peaks at 435 nm coordinate clearly indicate that the spectral intensity change of the 435 nm band occurs before those of the other bands at 415, 425, 475, 525, 535, 545, 555, and 635 nm. The bands at 415 and 425 nm are due to the Soret absorbance bands for OxyMb and MetMb (Swatland, 1989), while the bands at 525, 535, 545, and 555 nm originate from the diverse molecular surrounding of the OxyMb component (Liu & Chen, 2000). Therefore, the result implies that DeoxyMb fractions recover faster than the other components. In addition, it also suggests that intensity variation of the band around 575 nm occurs before the fluctuation in the band intensities at 475, 525, 535, 545, and 555 nm. The observation in Fig. 3B once again reveals the complexity of the band origins in visible region.

3.3. 2D Correlation spectra in the NIR region

Fig. 4a and b show, respectively, the synchronous and asynchronous 2D NIR correlation spectra of frozen meats thawing from 0 to 60 min. The synchronous spectrum reveals the presence of autopeaks and cross-peaks at 1175 and 1390 nm, which arise from the second overtones of C–H stretching modes and the combination band of the corresponding C–H vibration modes. In the asynchronous spectrum (Fig. 4b), cross-peaks show the asynchronocity between the 1410 nm band due to the O–H stretching vibration and the 1160 and 1355 nm bands ascribed to the C–H vibrations, and their signs indicate that the O–H fractions vary earlier than the C–H fractions. The fast variation of the O–H groups suggests that the melting of ice crystals existing in frozen meats precedes the relaxation of C–H groups.

Fig. 5a and b, respectively, present synchronous and asynchronous 2D NIR correlation spectra of frozen meats thawing from 75 to 180 min. A notable difference between Figs. 5a and 4a is the appearance of dominant autopeaks at 1450 and 1650 nm. The bands at 1450 and 1650 nm are ascribed to the first overtones of the O–H/N–H and C–H stretching modes respectively. Obvious intensity increase of the O–H/N–H modes appears to arise from the melting of ice crystals and the relaxation/proteolysis of meat proteins, whereas that of the C–H fractions appears to come from the relaxation of meat

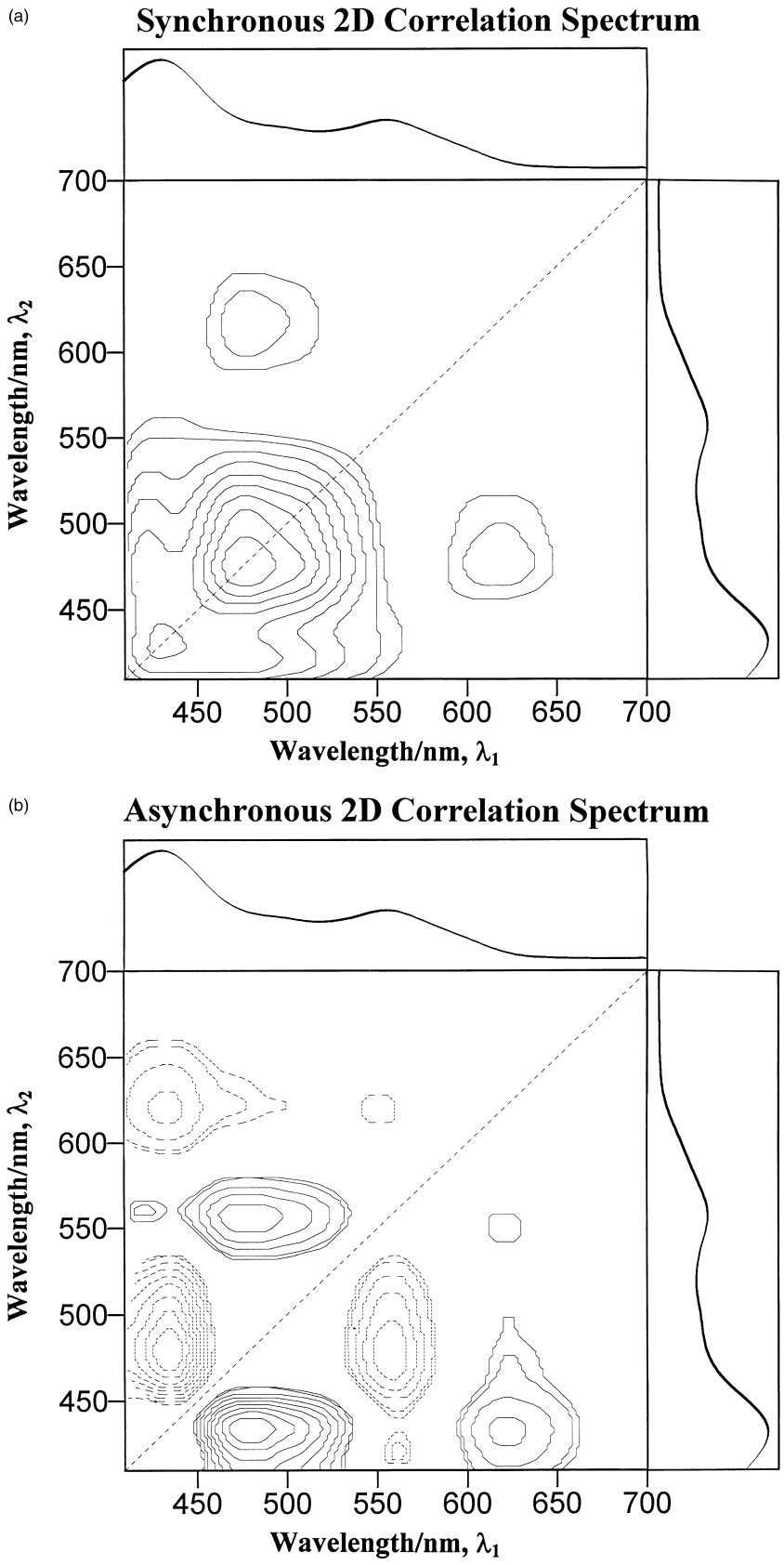

Fig. 2. 2D visible correlation spectra of frozen chicken meats thawed from 0 to 60 min. The average spectrum for the data set is plotted at the top and right of each plot: (a) synchronous spectrum: (b) asynchronous spectrum.

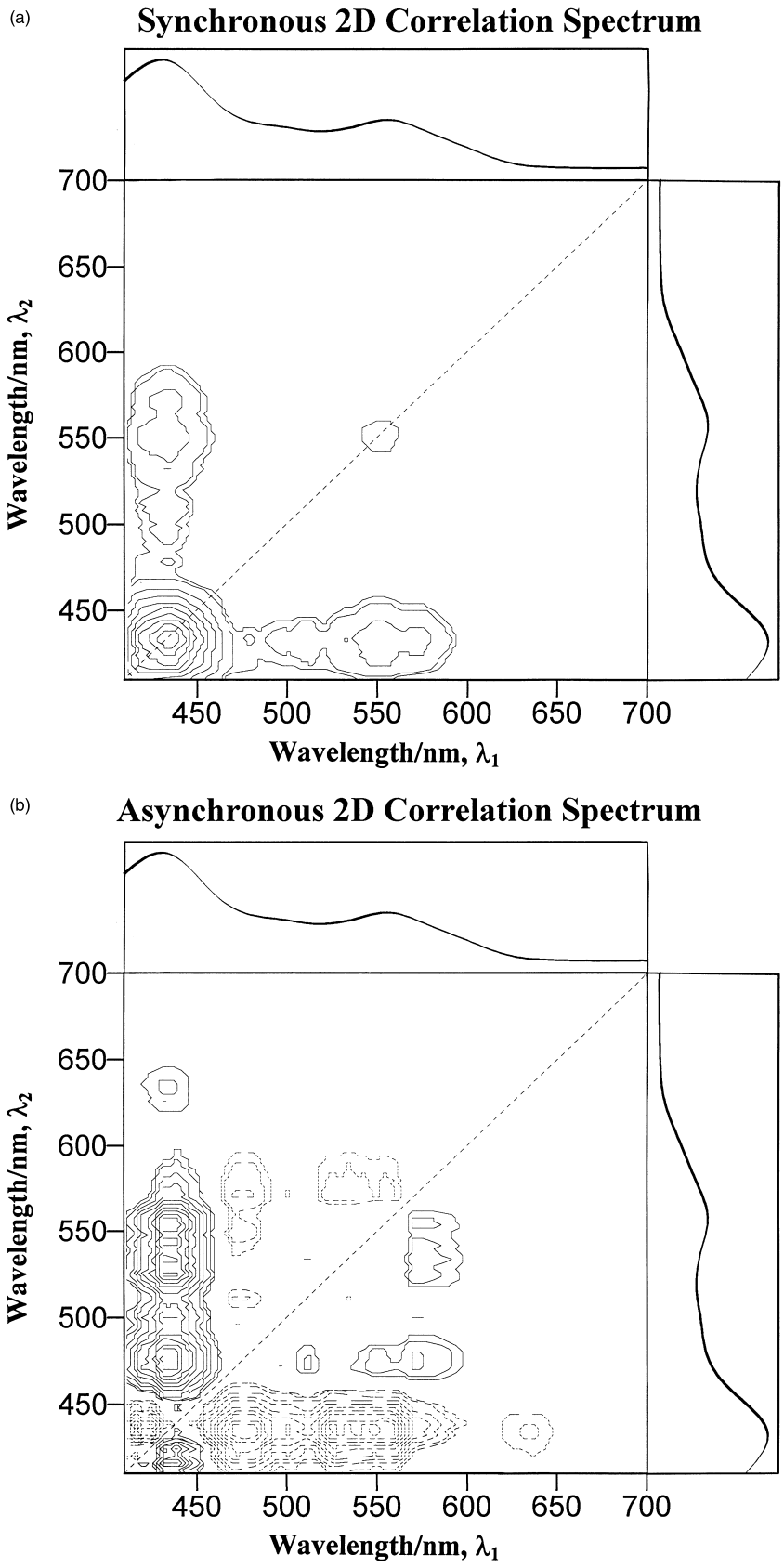

Fig. 3. 2D visible correlation spectra of frozen chicken meats thawed 75–180 min. The average spectrum for the data set is plotted at the top and right of each plot: (a) synchronous spectrum: (b) asynchronous spectrum.

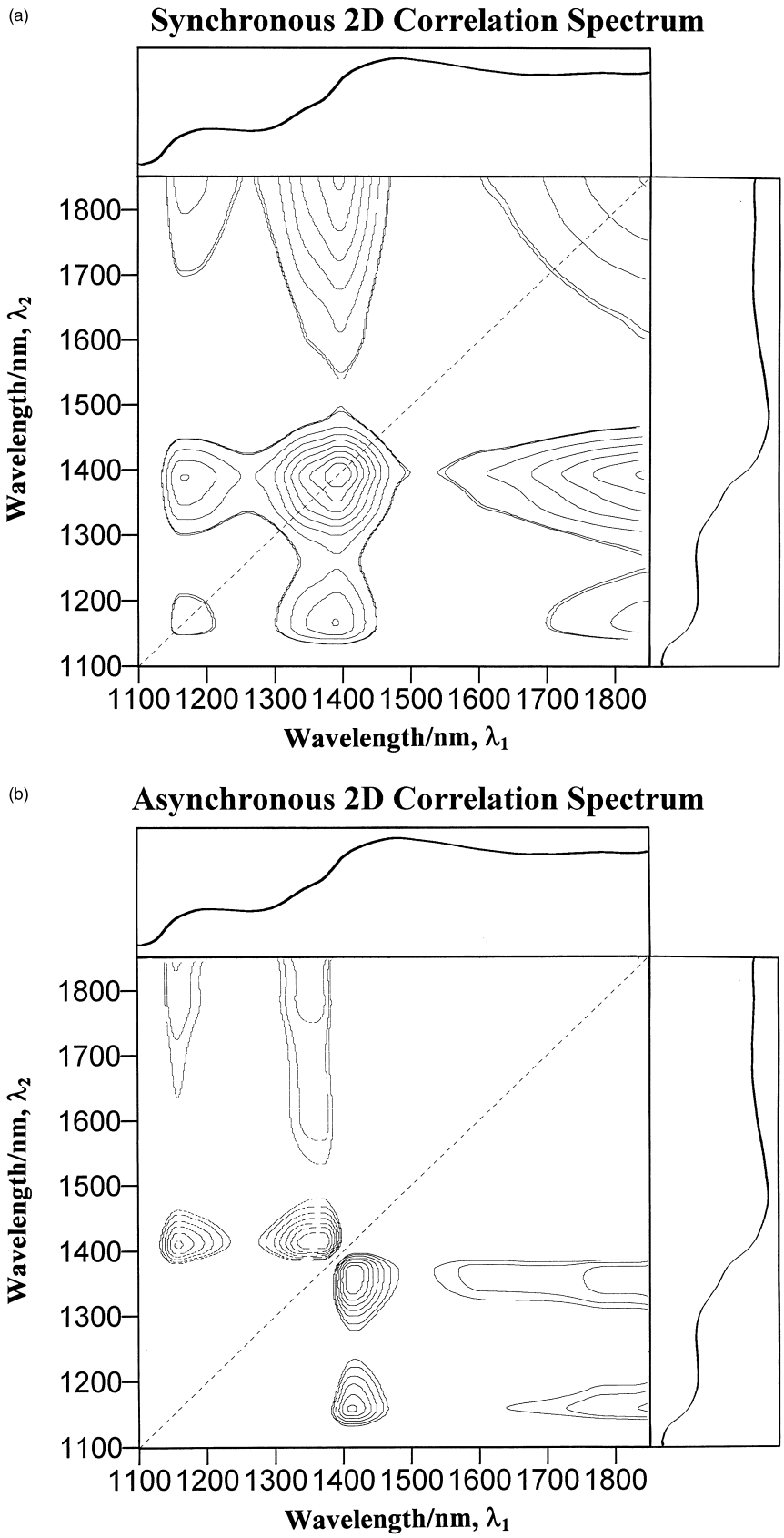

Fig. 4. 2D NIR correlation spectra of frozen chicken meats thawed from 0 to 60 min. The average spectrum for the data set is plotted at the top and right of each plot: (a) synchronous spectrum: (b) asynchronous spectrum.

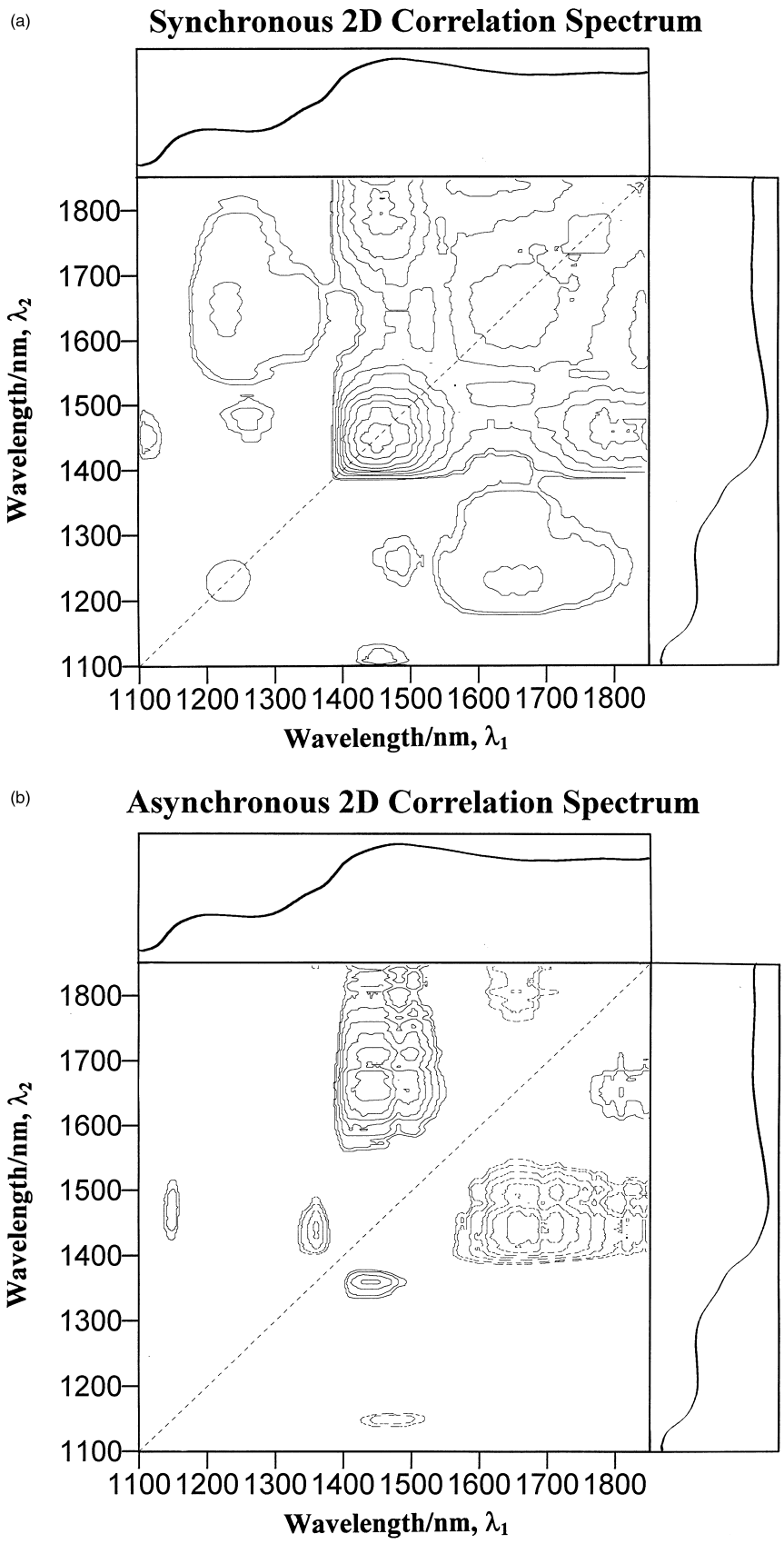

Fig. 5. 2D NIR correlation spectra of frozen chicken meats thawed 75–180 min. The average spectrum for the data set is plotted at the top and right of each plot: (a) synchronous spectrum: (b) asynchronous spectrum.

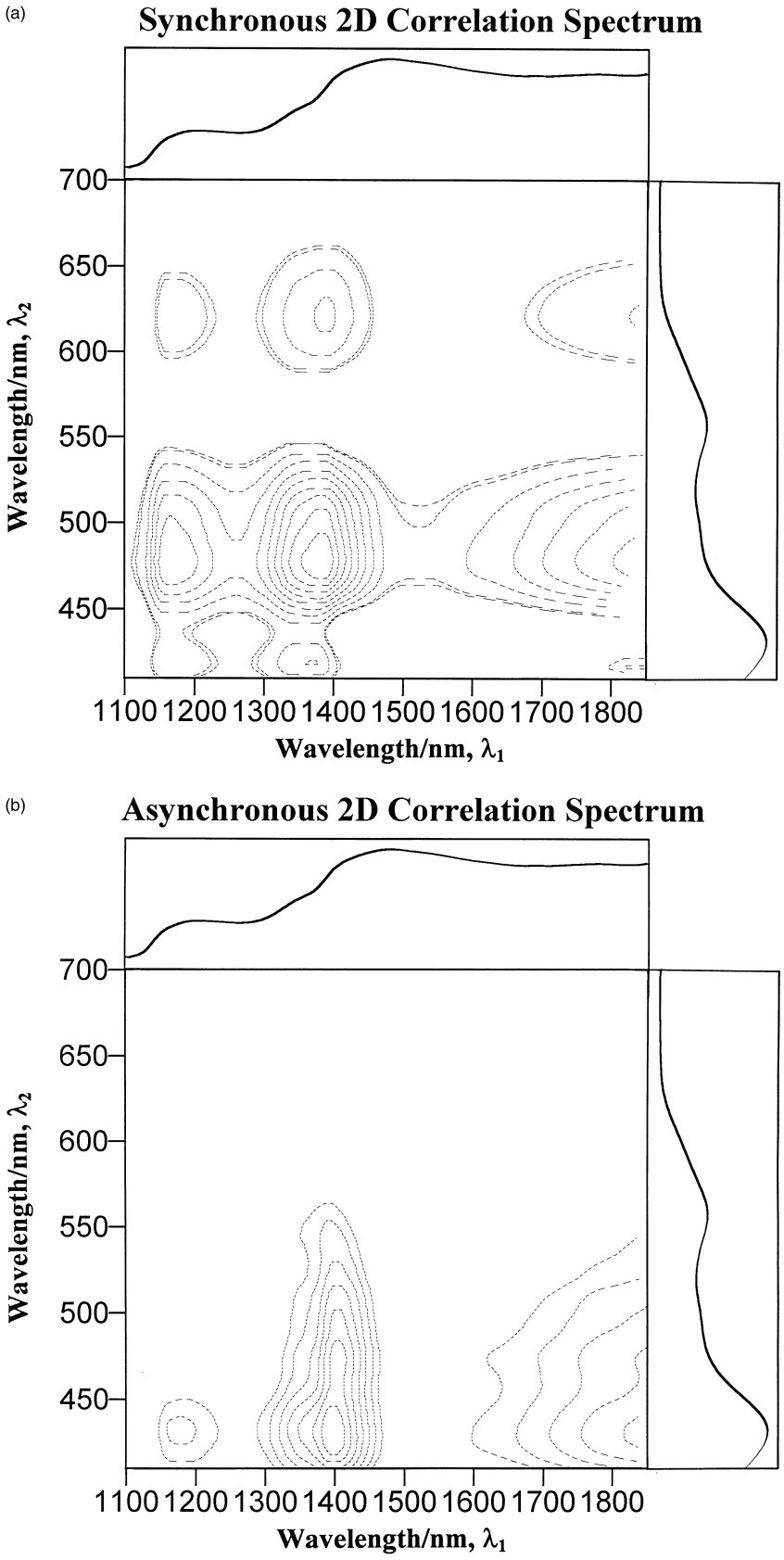

Fig. 6. 2D correlation spectra of frozen chicken meats thawed from 0 to 60 min in the off-diagonal region bounded by 410–700 nm (vertical) and 1100–1850 nm (horizontal). The corresponding portions of the average spectrum for the data set are plotted at the top and right of each plot: (a) synchronous spectrum: (b) asynchronous spectrum.

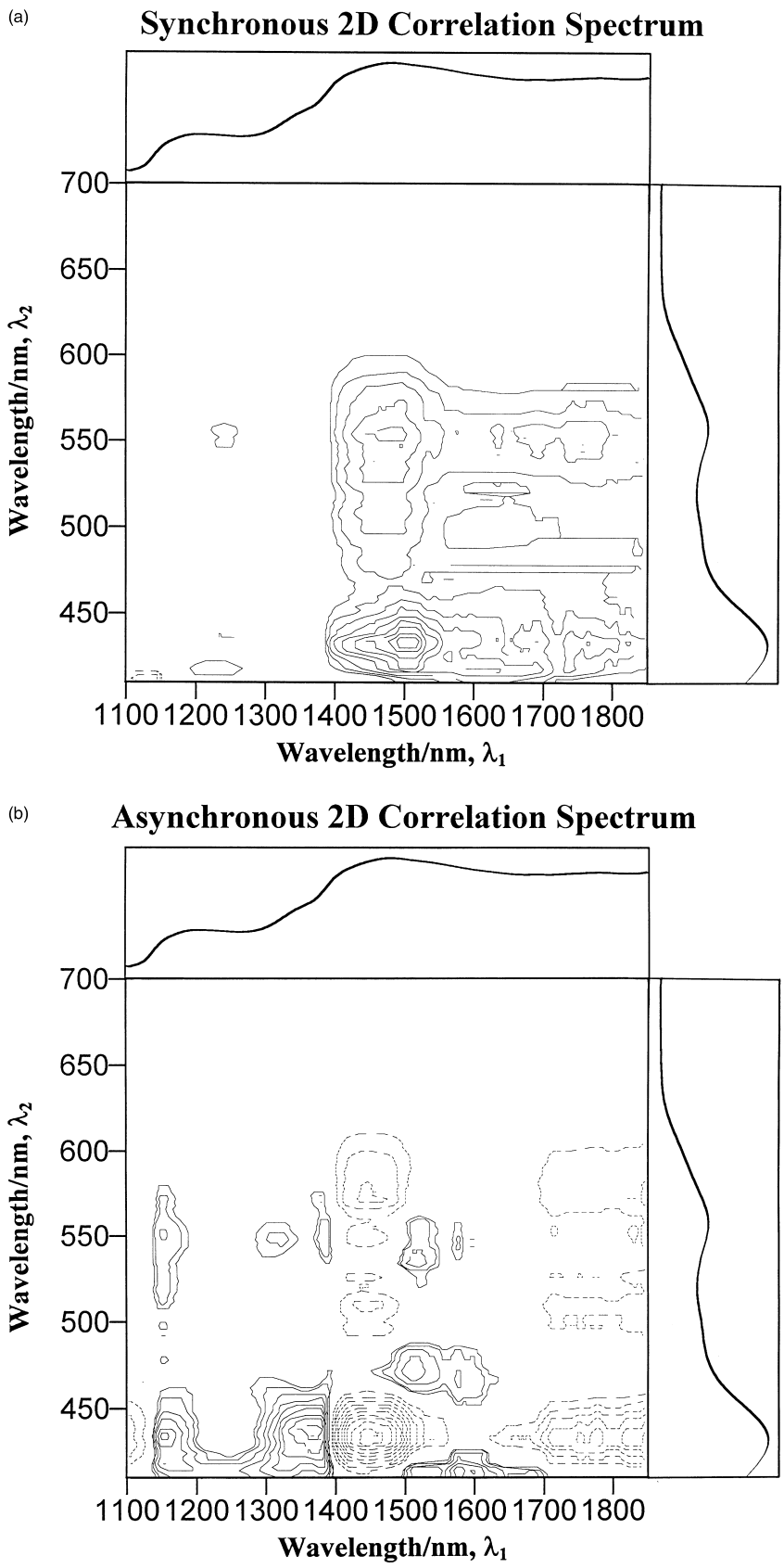

Fig. 7. 2D correlation spectra of frozen chicken meats thawed 75–180 min in the off-diagonal region bounded by 400–700 nm (vertical) and 1100–1850 nm (horizontal). The corresponding portions of the average spectrum for the data set are plotted at the top and right of each plot: (a) synchronous spectrum: (b) asynchronous spectrum.

lipids. The asynchronous spectrum shown in Fig. 5b reveals that the intensity change at the 1435 and 1485 nm bands, due to the O–H and N–H stretching modes of water and proteins, occurs before the NIR bands at 1355 and 1650 nm, ascribed to C–H groups. Consequently, the observation in Fig. 5b, alone with Fig. 4b, suggests the significant coordination process for the hydrophilic O–H and N–H groups in meats, exclusively hydrophobic C–H fraction.

Notably, there are cross-peak shifts from the peak at 1410 nm (Fig. 4b) to peaks at 1435 and 1485 nm (Fig. 5b) as well as at 1450 nm (Fig. 5a). It suggests the following possibilities: within the initial thawing, the amount of free water species increases due to the melting of ice crystals; and with the thawing continuing, free water molecules begin to form self-association and to interact with other components such as proteins and fatty acids through hydrogen bonding, and at the same time, proteins undergo relaxation and proteolysis. Therefore, the 1410, 1435, and 1450 nm bands can be assigned to the first overtones of the O–H stretching modes for free water species, self-associated water species, and water complexes (i.e. the interaction of water with proteins through hydrogen bonding), and the 1485 band is assigned to the first overtone of the N–H stretching mode of proteins (Osborne et al., 1993).

Undoubtedly, the NIR bands discussed above include the contributions from other meat components. For example, cell membrane phospholipids may absorb at the observed O–H and N–H wavelengths, and the peptide backbone of proteins contributes to C–H bands. But, in general, their effects on spectral characterization are minimal due to lower concentration.

3.4. 2D Heterospectral correlation spectra of the bands in visible and NIR ranges

The 2D correlation spectra of the visible and NIR absorption bands are given in Figs. 6 and 7 for the 0–60 and 75–180 min thawing, respectively. Strong negative synchronous cross-peaks in Fig. 6a reveal that the decrease in the spectral intensity of the visible bands at 420, 475, and 620 nm is clearly correlated with the spectral intensity increase of the NIR bands located at 1175 and 1375 nm. The signs of asynchronous cross-peaks in Fig. 6b indicate that the intensity increase at 435 nm band occurs before those at 1175 and 1390 nm. The result suggests that the relaxation of DeoxyMb component develops faster than that of the C–H groups. On the other hand, in conjunction with Fig. 4b, it is possible to conclude that the recovery of DeoxyMb species is synchronously accompanied by the melting of ice crystals.

Fig. 7a shows quite different correlation peaks from those in Fig. 6a. Positive synchronous cross-peaks reveal the similarity in intensity variation between the visible bands at 435 and 550 nm and the NIR bands at 1240, 1485, 1500, and 1750 nm. In the asynchronous spectrum (Fig. 7b), the signs of cross-peaks suggest that the intensity increase of the visible bands at 435 and 575 nm varies before those of the 1450 and 1750 nm NIR band, but after those at 1165 and 1385 nm. This means that the relaxation of DeoxyMb and OxyMb components occurs before the formation of water complexes, and after the relaxation of the C–H groups. The result in Fig. 7b seems to be in contradiction with the observation in Fig. 6b. However, both may reflect the physical, chemical, and biochemical changes occurring at different stages of meat thawing. In general, the recovery of meat color occurs before other developments, such as the relaxation of lipids and the relaxation/proteolysis of proteins.

4. Conclusions

The application of 2D correlation spectroscopy to the Vis/NIR spectral intensity variation associated with the thawing behavior of frozen chicken meats has detected the changes of not only three forms of myoglobin in the visible region but also the C–H and N–H/O–H fractions in the NIR region.

With limited exposure to atmospheric oxygen, the thawing increases the peak intensity at 435 and 555 nm probably due to the relaxation of DeoxyMb and OxyMb, respectively. The decreases at 475 nm (MetMb) and 620 nm (SulfMb) may be attributed to the decomposition of these two proteins into small molecules due to specific enzymes. Asynchronous 2D visible spectra indicate that the decomposition of MetMb and SulfMb species occurs before the relaxation of DeoxyMb and OxyMb, and also that the DeoxyMb species recover faster than the other components.

The appearance and intensity increase of a number of NIR bands accompanied with meat thawing indicate the involvement of complex physical, chemical, and biochemical changes during the process, for example, melting of ice crystals, relaxation of lipids, and relaxation/proteolysis of proteins. The asynchronous NIR spectra suggest that the intensity increase of the O–H/N–H fractions occurs earlier compared to the intensity increase of the C–H fractions. This implies that both the melting of ice crystals and the relaxation and proteolysis of proteins precede the relaxation of lipids. Also, the result implies the coordination process for hydrophilic O–H and N-H fractions.

The strong synchronous cross-peaks between the visible and NIR bands show that the intensity increases of the visible bands near 435 and 550 nm are positively correlated with those of the NIR bands at 1240, 1485, 1500, and 1750 nm, while the intensity decreases of the 425, 475, and 620 nm bands are negatively correlated

with the NIR bands at 1175 and 1375 nm. The asynchronous spectra suggest a complex mechanism for thawing. For example, the increase of the 435 and 555 nm bands occurs earlier than the increase of the C–H bands during the initial thawing, but later than that of the C–H groups after a prolonged thawing.

Acknowledgements

We wish to express our sincere thanks to Professor Y. Ozaki (Kwansei Gakuin University) and Dr. I. Noda (The Procter and Gamble Company, USA) for their valuable comments and suggestions.

References

Chen, H., & Marks, B. P. (1997). Evaluation previous thermal treatment of chicken patties by visible/near-infrared spectroscopy. *Journal of Food Science, 62*, 753–756,780.

Chen, H., & Marks, B. P. (1998). Visible/near-infrared spectroscopy for physical characteristics of cooked chicken patties. *Journal of Food Science, 63*, 279–282.

Chen, Y. R., Huffman, R. W., Park, B., & Nguyen, M. (1996). Transportable spectrophotometer system for on-line classification of poultry carcasses. *Applied Spectroscopy, 50*, 910–916.

Chen, Y. R., Park, B., Huffman, R. W., & Nguyen, M. (1998). Classification of on-line poultry carcasses with backpropagation neural networks. *Journal of Food Process Engineering, 21*, 33–48.

Fennema, O. R. (1996). *Food chemistry* (3rd ed.). New York: Marcel Dekker Inc.

Francis, F. J., & Clydesdale, F. M. (1975). *Food colorimetry: Theory and application*. New York: Chapman and Hall.

Kinsman, D. M., Kotula, A. W., & Breidemstein, B. C. (1994). *Muscle foods*. New York: Chapman and Hall.

Lawrie, R. A. (1985). *Meat science* (4th ed.). Oxford: Pergamon Press.

Liu, Y., & Chen, Y. R. (2000). Two-dimensional correlation spectroscopy study of visible and near-infrared spectral intensity variations of chicken meats in cold storage. *Applied Spectroscopy, 54*, 1458–1470.

Liu, Y., Chen, Y. R., & Ozaki, Y. (2000a). Two-dimensional visible/near-infrared correlation spectroscopy study of thermal treatment of chicken meats. *Journal of Agriculture and Food Chemistry, 48*, 901–908.

Liu, Y., Chen, Y. R., & Ozaki, Y. (2000b). Characterization of visible spectral intensity variations of wholesome and unwholesome chicken meats with two-dimensional correlation spectroscopy. *Applied Spectroscopy, 54*, 587–594.

McElhinney, J., Downey, G., & Fearn, T. (1999). Chemometric processing of visible and near infrared reflectance spectra for species identification in selected raw homogenized meats. *Journal of Near Infrared Spectroscopy, 7*, 145–154.

Noda, I. (1993). Generalized two-dimensional correlation method applied to infrared, Raman, and other types of spectroscopy. *Applied Spectroscopy, 47*, 1329–1336.

Osborne, B. G., Fearn, T., & Hindle, P. H. (1993). *Practical near-infrared spectroscopy with application in food and beverage analysis* (2nd ed.). New York: John Wiley & Sons.

Price, J., & Schweigert, B. (1987). *The science of meat and meat products* (3rd ed.). Connecticut: Food and Nutrition Press.

Rannou, H., & Downey, G. (1997). Discrimination of raw pork, chicken and turkey meat by spectroscopy in the visible, near- and mid-infrared ranges. *Analytical Communications, 34*, 401–404.

Swatland, H. J. (1989). A review of meat spectrophotometry (300 to 800 nm). *Canadian Institute of Food Science and Technology Journal, 22*, 390–402.

Voet, D., & Voet, J. G. (1995). *Biochemistry* (2nd ed.). New York: John Wiley & Sons Inc.

Williams, P., & Norris, K. (1990). *Near-infrared technology in the agricultural and food industrious*. MN: American Association of Cereal Chemist.